



# Mass concentration intercomparison of soot generated with Mini-Cast

Benoît Sagot<sup>1</sup>, Guillaume Pailloux<sup>2</sup>, Amel Kort<sup>2</sup>

<sup>1</sup> ESTACA, ESTACA'Lab - Paris Saclay, Montigny-Le-Bretonneux, F-78180, France

<sup>2</sup> Autorité de Sûreté Nucléaire et de Radioprotection (ASNR), PSN-RES/SCA/LPMA, F-91400, Saclay, France

5 *Correspondence to:* Benoît Sagot (Benoit.sagot@estaca.fr)

**Abstract.** This study focuses on measuring mass concentration of soot aggregates generated with a Mini-CAST burner. The experiments were performed in a test bench able to generate soot particles with different size distributions and different OC/TC ratios. With this soot production, we assessed the mass concentration measurements based on three online instruments (TEOM, PPS and MA300) and two offline concentration determination (OC/TC and SMPS), considering the gravimetric measurement as a reference. The findings demonstrate that the TEOM and the quantification based on the thermo-optical OC/TC analyser performed within acceptable limits of 10 % in comparison to the gravimetric reference measurement, over a wide range of OC/TC, mass concentration and size distribution. The Pegasor Particle Sizer (PPS) mass concentration measurement which is based on the aerosol electrical charging is calibrated for a reference size distribution, and we suggested a correction of the mass concentration measurement based on the aerosol Fuchs active surface, that proved to be efficient within the limits of this study. Finally, we confirmed that the mass concentration measurements obtained with the MA300 aethalometer are OC/TC ratio and wavelength dependent, and we were able to establish OC/TC limits for the overall mass concentration evaluation with the infrared and ultraviolet wavelengths.

## 1 Introduction

In the context of studies on airborne dispersion of soot particles emitted during fire scenarios and monitoring and quantification of emissions from thermal engine, it is important to have a robust measurement of the mass concentration of emitted soot. These measurements are needed to assess the consequences of fires in Basic Nuclear Installations (Kort et al., 2022), as soot is responsible for clogging the last containment barrier made by HEPA filters, or for the metrology of conventional engines PM emissions (Aakko-Saksa et al., 2022). Dynamic real-time monitoring of mass emissions can be performed using various types of instruments based on different measurement principles, such as the real-time aethalometer-type measurement (MA300), the Tapered Element Oscillating Microbalances (TEOM) or the Pegasor Particle Sensor (PPS). These instruments allow the study of aerosols across a wide range of concentrations, from ambient air quality monitoring to highly concentrated exhaust emissions. The quantification performed by the PPS is based on the electrical charge on the surface of aerosols, making it extremely dynamic. However, it requires calibration that primarily depends on the median diameter of the aerosol particle size distribution. Similarly, the aethalometer is an instrument based on optical transmission through a soot cake collected on a filter, and its mass quantification is influenced by the physical nature of the soot, particularly the elemental carbon to organic



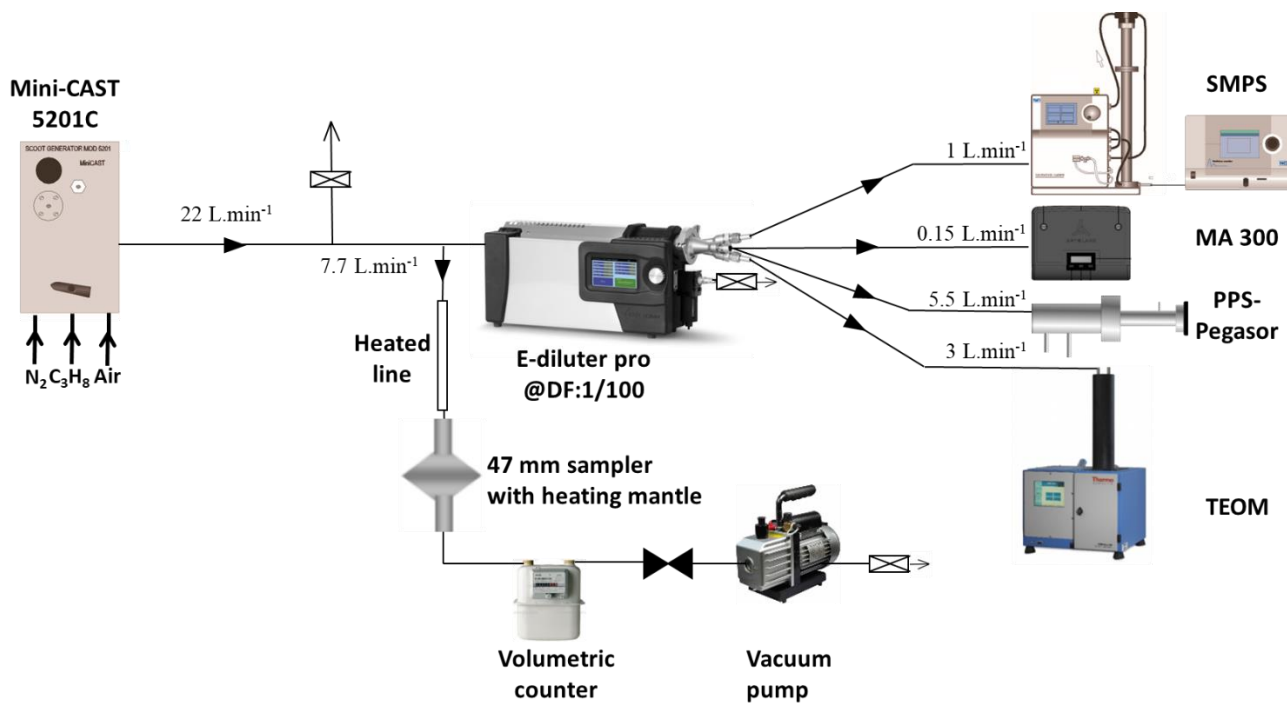
carbon ratio. For time stable emission sources, it is also possible to perform measurements using filter sampling, which allows mass concentration quantification either by weighing or through the Sunset Laboratory's OC/TC (Organic Carbon to Total Carbon ratio) analyser. All these mass concentration measurement techniques, usually used in different contexts, need to be qualified in an intercomparison to provide reliable and robust measurements.

35 For this purpose, soot was generated by a mini-CAST JING 5201C burner through the combustion of propane. Different studies have demonstrated that this mini-CAST generator can produce soot with a wide range of sizes and properties and is considered as a relevant tool to produce soot similar to those emitted by different combustion processes such as aircraft engine (Marhaba et al., 2019) or fire situation (Kort et al., 2021). It has been extensively utilized for soot characterization and as a time stable soot production source: by varying the gas flow rates supplied to this generator, it is possible to adjust the mass concentration  
40 over a wide range, as well as the particle size distribution and the elemental carbon to organic carbon ratio of the produced soot particles. The concentrations of soot generated are then either collected on a filter for ex-situ measurements or diluted using a double stage ejector-type diluter Dekati E-diluter, which delivers concentrations compatible with the measurement ranges of the instruments used.

The mass concentration evaluated by these online devices (MA300, PPS Pegasor, TEOM) were studied as a function of the  
45 mass concentration evaluated by a direct gravimetric measurement and considered as the reference measurement. The evaluation of the OC/TC ratio and the size distributions of the produced soot particles are also necessary for the interpretation of the instrument responses. A Scanning Mobility Particle Sizer (SMPS) was thus associated to the online instruments.

## 2 Experimental setup

For this experimental study we developed a test bench (Fig. 1) dedicated to the mass concentration intercomparison. This setup  
50 includes the soot generation source, the mini-CAST, followed by two heated lines maintained at 180°C. One line is used for filter sampling, while the other feeds a dilution system that distributes the diluted and cooled aerosol to various measurement instruments: the TEOM, PPS, MA300, and SMPS. The following sections detail the operating principles and implementation conditions of each component of this test setup.



55 **Figure 1 – Configuration of the experimental bench for intercomparison of mass concentration measurements**

The aerosol source is a Mini-CAST 5201C soot generator, which produces polydisperse soot particles by propane combustion. The principle of soot generation by the Mini-CAST involves an axial laminar diffusion flame, which is quenched by a cold, dry nitrogen flow to stop the combustion process and prevent soot oxidation. A rapid dilution with clean, dry air reduces the soot concentration, thereby limiting particle coagulation. By varying the flow rates of fuel, oxidizing air, and mixing nitrogen, it is possible to modify the characteristics of the flame, particularly its temperature, which affects both the quantity and the properties of the produced soot particles (Moore et al., 2014). As in the study by Marhaba et al. (Marhaba et al., 2019), propane flow is maintained at 60 mL/min, nitrogen flow at 0 mL/min, dilution air flow at 20 L/min and quenching nitrogen flow at 7 L/min. Variations of the soot production were obtained by varying the oxidation air flow rate from 0.9 L/min up to 1.5 L/min (0.9, 1, 1.15, 1.2, 1.25, 1.3, 1.35 and 1.5 L/min). The measurement points with oxidation air flow rate at 1, 1.15 and 1.5 L/min correspond respectively to the CAST3, CAST2 and CAST1 operating points in the study of Marhaba et al. (Marhaba et al., 2019). These specific operating points were also chosen for different studies (Bescond et al., 2016; Ouf et al., 2016). During the tests, stable generation points were sought, and before initiating filter sampling, the stability of the concentration production was ensured through measurements taken with online instruments such as the PPS and TEOM. Each measurement point was repeated three times, and the error bars represent the standard deviation of these measurements.

70 The first heated line connecting the mini-CAST soot generator to the filter sampler is maintained at 180°C and is dedicated to sampling on quartz fiber filters (Whatman quartz filter, Grade QM-H, diam. 47 mm), for ex-situ gravimetric measurements, and for later OC/TC analysis. These filters are used for mass quantification of soot concentration during stable generation



conditions. Quartz filters are preconditioned by heating at 180°C in an oven for one hour to eliminate moisture. They are then weighed and stored with desiccant to prevent reabsorption of humidity. During measurements, the filters are placed in the  
75 47 mm sampler with a 180°C temperature regulated heating jacket surrounding it. The collected mass is determined using a precision balance (Kern ABT 100-5M). The volume of gas passing through the filter is measured using a Gallus gas volumetric counter (see Fig 1.). Between the mass sampler and this Gallus volumetric counter, a heat exchanger cools the gas down to the ambient temperature, maintained at 20°C in the laboratory. By combining the collected mass with the measured gas volume, the soot mass concentration is calculated. This measurement is referred to as "Gravimetric mass concentration" in the study.

80 The second method for determining the mass concentration of generated soot is based on the Sunset Lab OC/TC field instrument (Sunset Laboratory), which has been used for both the measurement of the OC/TC ratio and the mass concentration. In this instrument, to separate the organic fraction of carbon (OC) from the elemental fraction (EC), the samples are subjected to various temperature plateaus (up to 850°C) in a helium inert atmosphere for the OC fraction and in an oxidizing atmosphere for the EC fraction. The gases formed are then transported by the helium flow to a catalytic furnace, where they are oxidized  
85 to CO<sub>2</sub>, then reduced to CH<sub>4</sub> for more accurate measurement by a calibrated Flame-Ionization Detector (FID). A thermo-optical correction is applied to separate OC from EC. The IMPROVE A protocol (Chow et al., 2001) has been used to reduce these pyrolytic conversions. OC/TC measurements have been performed on quartz fiber filters. Three punches of 1.5 cm<sup>2</sup> were analysed for each sample.

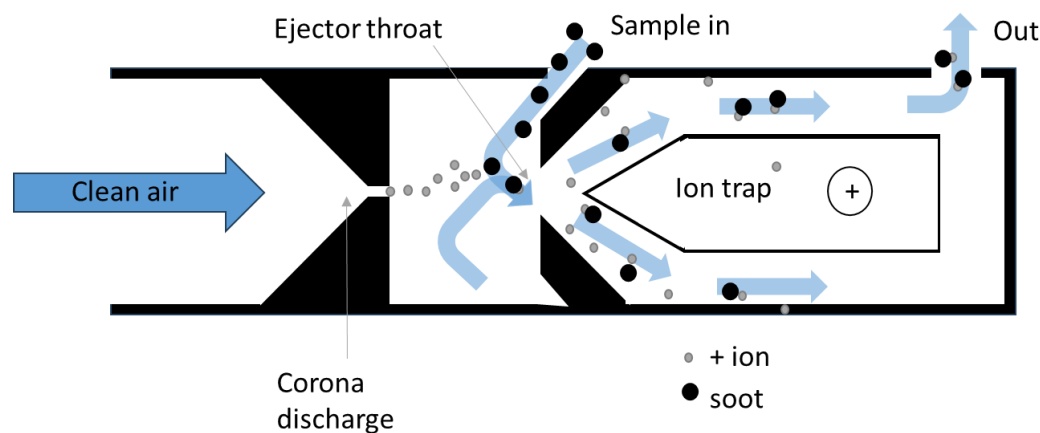
The second sampling line, after dilution, feeds real-time measurement instruments. The Dekati E-dilutor pro dilution system  
90 enables 2-stage dilution with a dilution factor set at 100. The first dilution stage is heated, while the second dilution stage operates at room temperature, where the aerosol sample is also cooled in a controlled manner. Both dilution stages are ejector-type, with a complementary sweep air flow in the duct. Concentrations downstream of the dilution system are compatible with the measurement ranges of the instruments used: a TEOM for a robust measurement of mass concentration, a PPS-Pegasor and a MA300 Aethalometer for real time mass concentration measurement and a SMPS for measurement of particle size  
95 distribution.

The TEOM (Thermo Scientific 1405) can continuously measure the mass of PM accumulating on a filter mounted upon an inertial microbalance using tapered element oscillating at its natural frequency (at 200 Hz). Aerosol is drawn in by a pump connected to the base of the microbalance. Sampled particles retained by the filter increase the mass of the oscillating system, producing a decrease in the natural frequency of vibration. Changes in the frequency of oscillation which are related to the  
100 mass of material accumulating on the filter are detected in quasi-real-time and converted by a microprocessor into an equivalent PM mass concentration (Allen et al., 1997). The sampled particles are heated at a temperature of 50°C.

The PPS is a real time sensor that can be used to provide the mass and number concentration of aerosols in the exhaust of car engine based on electrical measurement. The device is supplied with clean, dry compressed air. In the first phase, the clean air is ionized by the corona effect and ejected through an orifice (Ntziachristos et al., 2013). Particles are electrically charged by  
105 the binding of ions within a zone isolated by a Faraday cage. Only the small number of ions that charged the particles surface are lost to the sensor outlet where an electrometer is used to measure the "compensation" electrical current. It is related to the



particle number concentration and particle size, and (Ntziachristos et al., 2004) demonstrated this instrument provides a measure of the active surface area of the studied aerosol (Rostedt et al., 2014).



110 **Figure 2 – PPS operating principle**

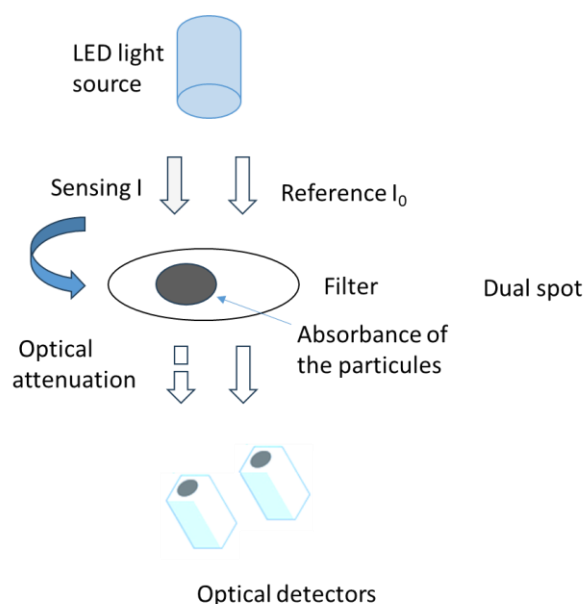
The raw current measurement is then used to determine the mass or number concentrations of sampled particles using calibration coefficients dependent on particle size. The remaining free ions with a high electrical mobility are eliminated by an ion trap.

The calibration factors for number and mass were determined by comparing the concentrations measured by the PPS on soot produced by a diesel engine at six different loads and rotational speed points (Ntziachristos et al., 2013) with those measured by reference instruments, a Dekati Electrical Low Pressure Impactor (ELPI) and a Scanning Mobility Particle Sizer (SMPS) for the number concentrations, and an AVL Micro Soot Sensor (MSS) for the mass concentration. For these six engine exhaust gas measurements points used to base the calibration, the average geometric mean diameter and standard deviation of the size distribution were respectively of 48 nm and 1.78 (Ntziachristos et al., 2013). Beyond this calibration on stabilized points, the temporal monitoring of engine mass concentration emissions during dynamic standardized driving cycles such as the WLTC (Worldwide harmonized Light-duty Test Cycle) demonstrated a very good correlation ( $R^2=0.96$ ) of this instrument, with another dynamic mass measurement instrument, the Micro Soot Sensor. This ability to track emissions dynamically (at Hz frequency) under high number and mass concentrations could be particularly useful for real-time emission monitoring in fire situations. Finally, the injector design protects the corona needle, and the charged particles are sensed with no need for contact with the sensor which can be beneficial in these polluted environments (Maricq, 2013).

The MA300 aethalometer (AethLabs, San Francisco) is a real time portable analyzer that uses the filter-based light absorption principle: the mass concentration measurement is based on the optical attenuation of a light beam passing through a cake of particles collected on a filtering fiber tape. The instrument draws a controlled flow through the collection spot on the filter tape, and when the light attenuation reaches a threshold value, the tape advances automatically. Filter-based light absorption techniques are subject to measurement artifacts due to scattering on the filter (Weingartner et al., 2003). In addition, real time



correction algorithms do not consider light absorption enhancement, at lower wavelengths due to light-absorbing organic components (Chakraborty et al., 2023). The instrument has five analytical channels that operate at different wavelengths (375, 470, 528, 625 and 880 nm), and the measurement of absorption at 880 nm is interpreted as Black Carbon (Hansen et al., 1984).



### 135 **Figure 3 – MA 300 operating principle**

One of the identified drawbacks of aethalometers is the overestimation of BC concentration on a new filter and the underestimation when the loading is high, with the most accurate concentrations being obtained on slightly loaded filters (Collaud Coen et al., 2010). Aethalometers based on the Dualspot™ technique use a double collection on two spots in parallel at different flow rates, to minimize this spot loading effects (Arnott et al., 2005; Drinovec et al., 2015). Aethalometers have  
140 been used to monitor black carbon concentrations in urban areas (Blanco-donado et al., 2022), assess biomass burning contribution to emissions in urban areas (Favez et al., 2007), or to measure personal exposure in working environment (Gren et al., 2022). However, the ability of aethalometers to accurately quantify soot emissions remains an active research topic. The recent study by (Aakko-Saksa et al., 2022) over a wide ship exhaust test matrix obtained with different fuels, engines, and emission control devices showed that measurement with an aethalometer could lead to overestimation of BC emissions.

### 145 **Results and discussion**

Fig. 4 shows the evolution of the Gravimetric mass concentration (left) and the number size distribution measured by the SMPS (right) as a function of oxidation air. When changing the oxidation air flow rate, the main parameter that vary is the fuel–air equivalence ratio  $\Phi$ , describing the flame in terms of fuel-lean ( $\Phi < 1$ ), stoichiometric ( $\Phi = 1$ ), and fuel-rich ( $\Phi > 1$ ) conditions (Marhaba et al., 2019).

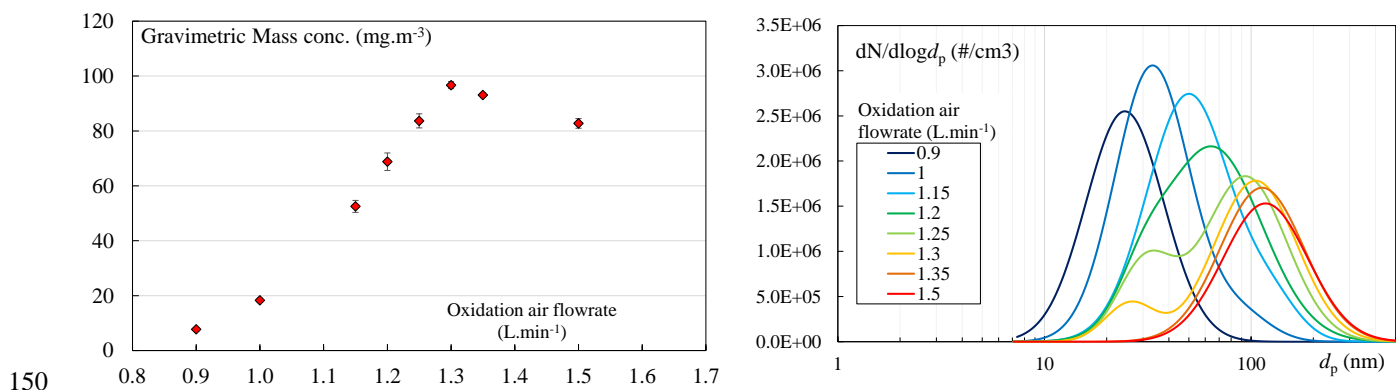


**Figure 4 – Evolution of the gravimetric mass concentration (left) and the number size distribution (right) as a function of oxidation air**

For oxidation air of 0.9 L.min<sup>-1</sup>, the size distribution of generated soot particles is monomodal with a number median diameter of 23.3 nm and the lowest mass concentration of 7.7 mg.m<sup>-3</sup>. (Moore et al., 2014) showed that by continuously increasing the oxidation air flowrate, the volumetric soot production reaches a maximum at a value close to 1.3 L/min when the adiabatic temperature of the flame reaches also its maximum, with a strong impact on the OC/TC organic-to-total carbon ratio. In our experiments, intermediate values of the oxidation air were thus added. When increasing the oxidation air flowrate, the produced mass concentration increases up to a maximum of 96.3 mg.m<sup>-3</sup> for soot generated corresponding to an oxidation air flowrate of 1.3 L.min<sup>-1</sup>. For this generation point, a bimodal size distribution is obtained. For higher oxidation airs, a decrease of the mass concentration is then observed. When reaching 1.5 L.min<sup>-1</sup>, the size distribution becomes monomodal again with the highest modal median diameter of 113.4 nm and a mass concentration of 82.8 mg.m<sup>-3</sup>. The measured particle size distributions were fitted with the sum of two log normal distributions that correspond to an ultrafine and a fine mode. We describe in Table 1 the nature of the distribution, and report, for each operating point, the median diameters of the two modes as well as their respective intensities expressed as a percentage. We also indicate the number median diameter of the measured distribution.

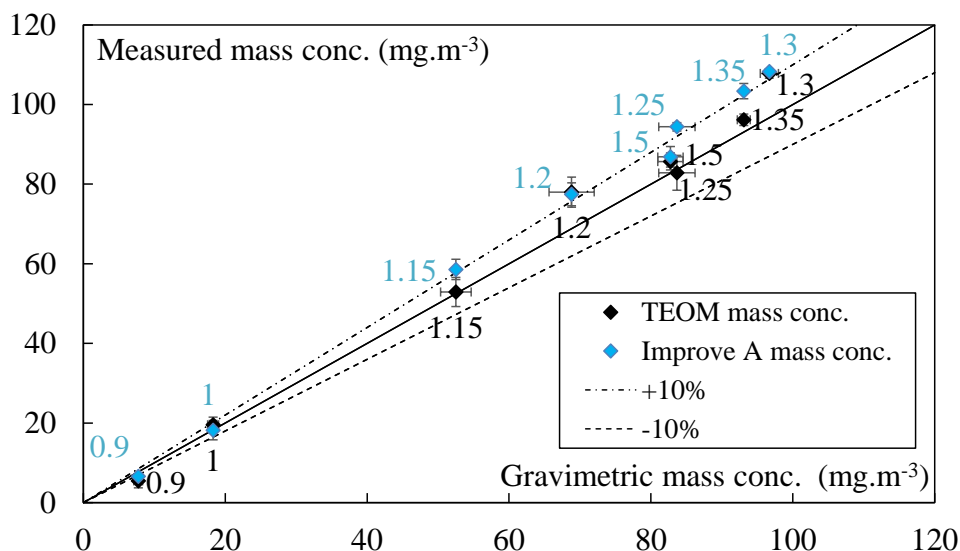
**Table 1 – Main characteristics of the number size distributions for each of the operating points studied**

Oxidation air (L.min <sup>-1</sup> )	Nature of the distribution	Mode 1 (nm)	Mode 2 (nm)	Number median diameter (nm)
0.9	monomodal	24.5 nm - 1%	(-)	23.3
1	bimodal	33.3 nm - 93%	90.5 nm - 7%	33.4
1.15	bimodal	49.9 nm - 92%	126.6 nm - 8%	51.4
1.2	bimodal	29.8 nm - 9%	64.7 nm - 91%	59.4
1.25	bimodal	31 nm - 25%	93.7 nm - 75%	73.7
1.3	bimodal	26 nm - 13%	105.2 nm - 87%	94.7
1.35	monomodal	(-)	113 nm - 100%	109.4



1.5	monomodal	(-)	117.3 nm - 100%	113.4
-----	-----------	-----	-----------------	-------

Fig. 5 shows a parity curve of mass concentrations measured by the TEOM and those measured by OC/TC analysis as a function of reference gravimetric measurements.



170

**Figure 5 – Parity curve of mass concentrations measured by the TEOM and by OC/TC analysis as a function of the reference measurements with gravimetry (Solid line is a guide to the eye).**

Over a two decades wide mass concentration range, both mass concentrations measured by the TEOM and by OC/TC analysis are within a 10% interval of the gravimetric reference mass concentration, for the eight values of oxidation air flowrates tested (value indicated next to each measuring point, in L.min<sup>-1</sup>).

175

Fig. 6 (left) shows the mass concentrations measured by the PPS, as a function of those measured gravimetrically for soot produced with the different oxidation air flow rates tested. Fig. 6 (right) shows the evolution of the mass concentration ratio measured by the PPS and gravimetrically as a function of the SMPS measured number median diameter. This ratio logically increases as the median diameter decreases. Indeed, the PPS estimates the particle mass based on their active surface area (Ntziachristos et al., 2004). For spherical particles with a constant diameter, the mass is proportional to the cube of the particle diameter, while the surface area scales with the square of the diameter, resulting in a surface-to-mass ratio that varies as 1/Diameter. With the calibration performed on a polydisperse soot aerosol produced by an engine, the mass is correctly estimated for median diameters close to 80 nm.

180

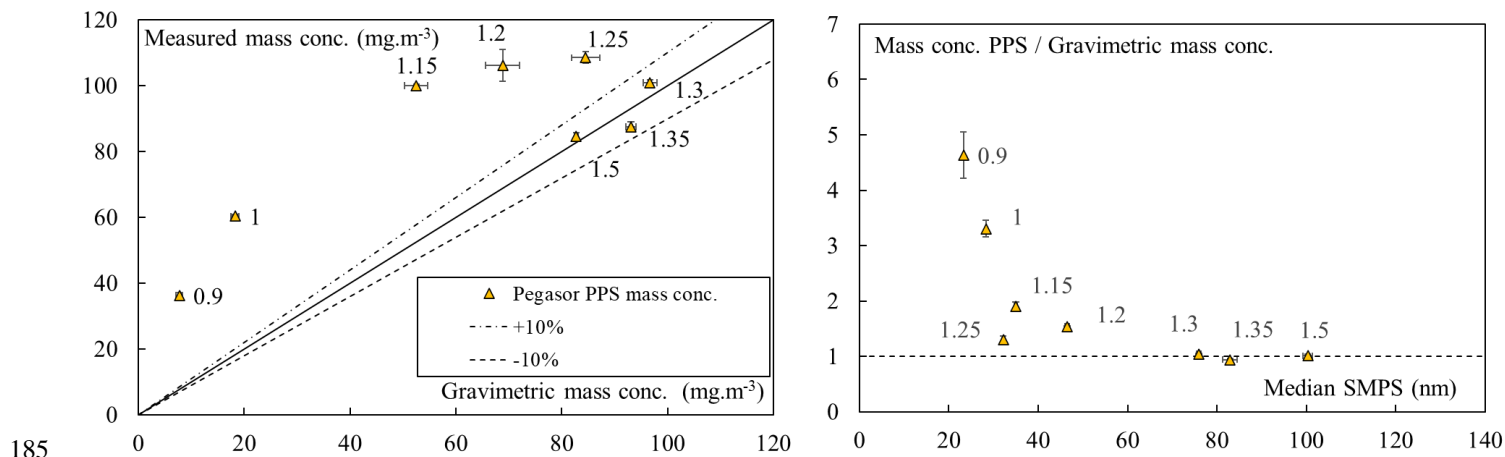


**Figure 6** –Mass concentrations measured by the PPS-Pegasor as a function of the reference measurements with gravimetry (left) and ratio of mass concentration measured by PPS and TEOM as a function of the median diameter

The PPS measurement using becomes reliable for soot generated with an oxidation air flowrate between 1.3 L/min and 1.5 L/min, where the mass concentration ratio measured by PPS and gravimetrically is independent from the measured median diameter. The mass concentration  $C_{m,PPS\ raw}$  results have been corrected using Eq. (1) (Pandis et al., 1991):

$$C_{m,PPS\ corrected} = C_{m,PPS\ raw} \cdot \left( \frac{d_{s,Fuchs}}{d_0} \right)^{x(d_p)} \quad (1)$$

With  $d_{s,Fuchs}$  the diameter of Fuchs active surface, evaluated from the size distribution for each measurement points ( $d_{s,Fuchs}$  evaluated values are reported in table 2),  $x(d_p) = 1.39$  in the transition regime (30 nm to 150 nm) (Jung and Kittelson, 2005), and  $d_0$  a reference diameter taken arbitrarily equal to 100 nm.

We also calculated the mass concentration based on the number size distribution measured by the SMPS. For this evaluation, we considered a so-called true density for the aggregates that varies depending on the considered point. Indeed, as reported by several studies (Ouf et al., 2019; Park et al., 2004), the density of combustion soot particles decreases when the organic fraction increases, from the value of the elemental carbon density  $\rho_{EC}$  (close to 2000 kg.m<sup>-3</sup>), down to the value of the organic carbon density  $\rho_{OC}$ . For diesel soot particles, Park et al. (2004) proposed to evaluate the true aggregate density through a mixing law based on the mass fraction of organic carbon ( $x = M_{OC} / (M_{OC} + M_{EC})$ ),  $\rho_{EC}$  and  $\rho_{OC}$  the respective density of elemental and organic carbon, and expressed as:

$$\rho_{true} = \frac{1}{\frac{x}{\rho_{OC}} + \frac{1-x}{\rho_{EC}}} \quad (2)$$

Based on data from a wide range of liquid, gaseous or solid fuel combustion soot, (Ouf et al., 2019) suggested that a constant true density could be considered with a mean value of  $\rho_{EC} = 1834$  kg.m<sup>-3</sup> for soot with OC contents below 5%. In the absence of metallic compounds which is the case for the Mini-CAST soot, they also proposed considering three different ranges of the true density, as a function of  $x$ , the organic carbon to total carbon ratio: For low OC contents (i.e. below 5%) and high OC contents (i.e. above 20%), they consider respective constant true density values  $\rho_{EC}$  and  $\rho_{OC}$ . For intermediate OC content

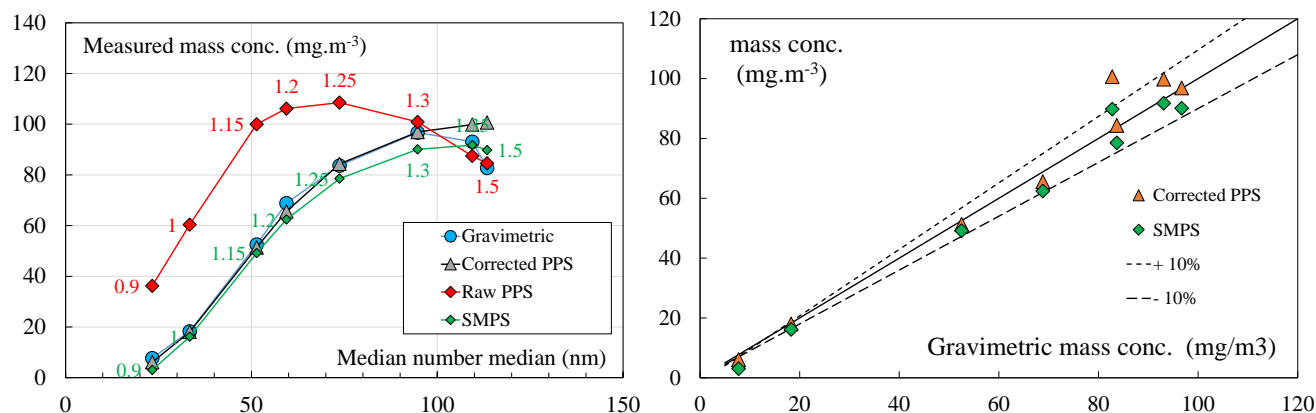


values between these two reference points, a linear mixing law as a function of  $x$  is suggested by (Ouf et al., 2019). Using this zone-based approach, we observed an underestimation of soot mass for almost all measurement points. Therefore, we considered using the Park mixing model (Eq. 2), with the values  $\rho_{EC} = 1834 \text{ kg.m}^{-3}$  for  $x=0$ , and  $\rho_{OC} = 1285 \text{ kg.m}^{-3}$ , as suggested by (Ouf et al., 2019). We report in table 2 the values obtained for the OC/TC ratios as determined by thermo-optical analysis and the corresponding evaluated true densities, that were used to evaluate the SMPS mass concentrations reported on Fig. 7. The measured values of the OC/TC organic fraction contained in soot compare well with those obtained in the previous study by (Marhaba et al., 2019) for equivalent operating conditions of the Mini-CAST. For the considered points (CAST3: 1 L/min, CAST2: 1.15 L/min and CAST1: 1.5 L/min of oxidation airflow), (Marhaba et al., 2019) reported OC/TC ratio values of 87%, 46.8% and 4.1%, respectively, while we measured corresponding OC/TC values of 56.7%, 46 % and 6.2%. Indeed, as highlighted by (Moore et al., 2014), soot production conditions can vary with parameters other than the overall carbon/oxygen ratio of the flame, and variations in mode size or OC/TC ratio have already been observed between different studies using different Cast or Mini-CAST generators. This makes it difficult to directly compare OC/TC data between studies conducted with this type of generator and justify the necessity to carry out the thermo-optical analysis of the organic content of the soot.

**Table 2 – Properties and true density of considered emitted soot particles**

Oxidation air ( $\text{L.min}^{-1}$ )	OC/TC	$d_{s,Fuchs}$ (nm)	True density ( $\text{kg.m}^{-3}$ )
0.9	68.2%	28	1420
1	56.7%	42	1476
1.15	46.0%	62	1533
1.2	43.3%	71	1548
1.25	37.7%	83	1580
1.3	24.3%	97	1662
1.35	22.7%	110	1672
1.5	6.2%	113	1787

As can be observed on Fig. 7, for the mass concentrations determined from SMPS size distributions and the true density, as well as for the evaluations based on the corrected PPS, we observe good agreement with the mass concentration obtained from the gravimetric measurement: except for a very limited number of points and at very low mass concentration measurements, both mass concentrations evaluated from the SMPS and by the PPS after correction fall within a 10% interval of the gravimetric reference mass concentration.



230 **Figure 7 – Comparison of gravimetric mass concentrations with evaluations based on PPS and SMPS measurements.**

Fig. 8 (left) shows the mass concentrations measured by the MA 300 for ultraviolet and infrared wavelengths, as a function of those measured by the gravimetric method for soot produced with the different oxidation air flow rates tested (value indicated next to each measuring point, in L.min<sup>-1</sup>). Fig. 8 (right) shows the evolution of the OC/TC ratio as a function of the oxidation air flowrate. For oxidation air of 0.9 L.min<sup>-1</sup>, the soot generated is 68% composed by organic carbon. This percentage drops to around 6% for those generated with 1.5 L.min<sup>-1</sup> oxidation air.

235

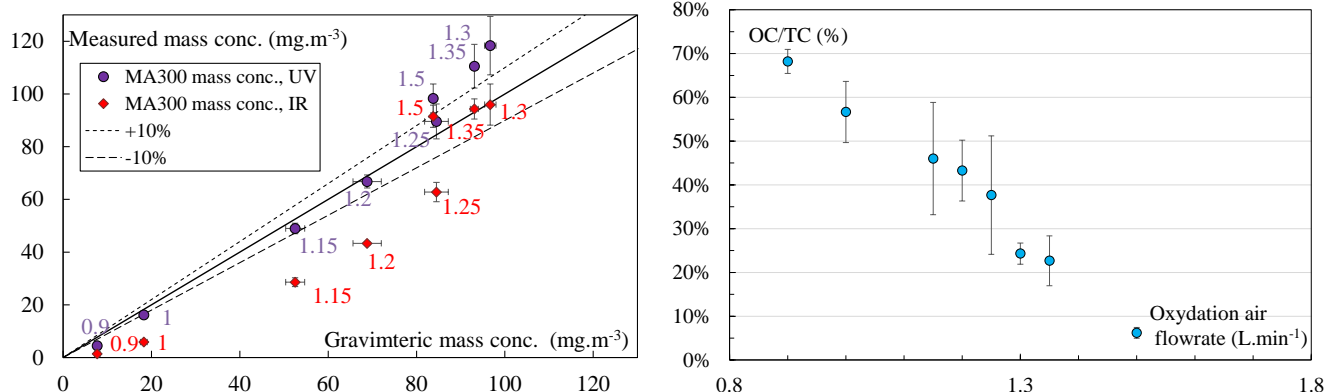


**Figure 8 – Mass concentrations measured by the MA300 as a function of the reference measurements with gravimetry**

The MA 300 measurement becomes reliable at infrared wavelengths for soot generated with an oxidation air flow rate of between 1.3 L/min and 1.5 L/min, which are soot particles predominantly made up of elemental carbon (less than 24% of OC). For ultraviolet wavelengths, measurements are reliable for soot generated with oxidation airflows of less than 1.3 L/min, and therefore with high organic carbon ratios, at least higher than 38%.

240



## Conclusion

For this intercomparison of instruments and measurement techniques for the evaluation of the soot mass concentration, we used a Mini-CAST generator commonly employed in laboratory experiments to produce soot particles under stable and controlled conditions. This generator allows to generate soot representative of that emitted by internal combustion engines, as well as in fire situations or during biomass combustion. By significantly and continuously varying one of the Mini-CAST parameters, we were able to generate a set of eight soot particles measurement points, with significant variations in the organic to total carbon ratio OC/TC, ranging from 6% to 68%, as well as in their size distributions, while also achieving mass concentrations covering values from 7 to 96 mg·m<sup>-3</sup>. Over almost two decades of mass concentration range, we obtained a very good correlation between the gravimetric method using filter sampling, the real-time online methods with the reference TEOM instrument, and the offline thermo-optical analysis, which also provided access to the OC/TC fraction. Based on the electrical charging of the aerosol particles, the Pegasor Particle Sensor (PPS) analyser provides a real-time measurement of the mass concentration at one Hertz frequency, but with a response that depends on the particle size distribution. We established that with an appropriate correction based on the aerosol active surface, it can also provide relevant quantitative information on the soot mass concentration. Finally, the MA300 aethalometer was evaluated over a wide range of OC/TC ratios. In this instrument, the measurement technique is based on the attenuation of a light beam with different wavelength through a particle cake accumulating on a filter. This attenuation is dependent on the wavelength, and on the OC/TC ratio. We were able to determine a limit in soot organic content, with a maximum value of OC/TC=24% for which the infrared measurement allows quantification of the total mass concentration, rather than only the so-called "black carbon" fraction. We also established that the ultraviolet wavelength usually used to quantify brown carbon can also provide an evaluation of the total mass concentration, when the organic carbon ratios is sufficiently high, at least higher than 38%. When evaluating the soot mass concentration based on both the SMPS size distribution and a true density, we pointed out the lack of a general model for this parameter as a function of the OC/TC ratio in the literature.

## References

- 265 Aakko-Saksa, P., Kuittinen, N., Murtonen, T., Koponen, P., Aurela, M., Järvinen, A., Teinilä, K., Saarikoski, S., Barreira, L. M. F., Salo, L., Karjalainen, P., Ortega, I. K., Delhaye, D., Lehtoranta, K., Vesala, H., Jalava, P., Rönkkö, T., and Timonen, H.: Suitability of different methods for measuring black carbon emissions from marine engines, *Atmosphere (Basel)*, 13, <https://doi.org/10.3390/atmos13010031>, 2022.
- 270 Allen, G., Sioutas, C., Koutrakis, P., Reiss, R., Lurmann, F. W., and Roberts, P. T.: Evaluation of the TEOM® Method for Measurement of Ambient Particulate Mass in Urban Areas, *J. Air Waste Manag. Assoc.*, 47, 682–689, <https://doi.org/10.1080/10473289.1997.10463923>, 1997.



- 275 Arnott, W. P., Hamasha, K., Moosmüller, H., Sheridan, P. J., and Ogren, J. A.: Towards aerosol light-absorption measurements with a 7-wavelength aethalometer: Evaluation with a photoacoustic instrument and 3-wavelength nephelometer, *Aerosol Sci. Technol.*, 39, 17–29, <https://doi.org/10.1080/027868290901972>, 2005.
- 280 Bescond, A., Yon, J., Ouf, F. X., Rozé, C., Coppalle, A., Parent, P., Ferry, D., and Laffon, C.: Soot optical properties determined by analyzing extinction spectra in the visible near-UV: Toward an optical speciation according to constituents and structure, *J. Aerosol Sci.*, 101, 118–132, <https://doi.org/10.1016/j.jaerosci.2016.08.001>, 2016.
- Blanco-donado, E. P., Schneider, I. L., Artaxo, P., Lozano-osorio, J., Portz, L., and Oliveira, M. L. S.: Geoscience Frontiers Source identification and global implications of black carbon, *Geosci. Front.*, 13, 101149, <https://doi.org/10.1016/j.gsf.2021.101149>, 2022.
- 285 Chakraborty, M., Giang, A., and Zimmerman, N.: Performance evaluation of portable dual-spot micro-aethalometers for source identification of black carbon aerosols: Application to wildfire smoke and traffic emissions in the Pacific Northwest, *Atmos. Meas. Tech.*, 16, 2333–2352, <https://doi.org/10.5194/amt-16-2333-2023>, 2023.
- 290 Chow, J. C., Watson, J. G., Crow, D., Lowenthal, D. H., and Merrifield, T.: Comparison of IMPROVE and NIOSH Carbon Measurements, *Aerosol Sci. Technol.*, 34, 23–34, <https://doi.org/10.1080/02786820119073>, 2001.
- Collaud Coen, M., Weingartner, E., Apituley, A., Ceburnis, D., Fierz-Schmidhauser, R., Flentje, H., Henzing, J. S., Jennings, S. G., Moerman, M., Petzold, A., Schmid, O., and Baltensperger, U.: Atmospheric Measurement Techniques Minimizing light absorption measurement artifacts of the Aethalometer: evaluation of five correction algorithms, *Atmos. Meas. Tech.*, 457–474 pp., <https://doi.org/https://doi.org/10.5194/amt-3-457-2010>, 2010.
- 295 Drinovec, L., Močnik, G., Zotter, P., Prévôt, A. S. H., Ruckstuhl, C., Coz, E., Rupakheti, M., Sciare, J., Müller, T., Wiedensohler, A., and Hansen, A. D. A.: The “dual-spot” Aethalometer: An improved measurement of aerosol black carbon with real-time loading compensation, *Atmos. Meas. Tech.*, 8, 1965–1979, <https://doi.org/10.5194/amt-8-1965-2015>, 2015.
- 300 Favez, O., Cachier, H., Sciare, J., and Le Moullec, Y.: Characterization and contribution to PM<sub>2.5</sub> of semi-volatile aerosols in Paris (France), *Atmos. Environ.*, 41, 7969–7976, <https://doi.org/10.1016/j.atmosenv.2007.09.031>, 2007.
- 305 Gren, L., Kraus, A. M., Assarsson, E., Broberg, K., Engfeldt, M., Lindh, C., Strandberg, B., Pagels, J., and Hedmer, M.: Underground emissions and miners’ personal exposure to diesel and renewable diesel exhaust in a Swedish iron ore mine, *Int. Arch. Occup. Environ. Health*, 95, 1369–1388, <https://doi.org/10.1007/s00420-022-01843-x>, 2022.



- Hansen, A. D., Rosen, H., and Novakov, T.: The aethalometer – An instrument for the real-time measurement of optical  
310 absorption by aerosol particles, *Sci. Total Environ.*, 36, 191–196, <https://doi.org/36, 191–196>, [https://doi.org/10.1016/0048-9697\(84\)90265-1](https://doi.org/10.1016/0048-9697(84)90265-1), 1984, 1984.
- Jung, H. and Kittelson, D. B.: Characterization of aerosol surface instruments in transition regime, *Aerosol Sci. Technol.*, 39,  
902–911, <https://doi.org/10.1080/02786820500295701>, 2005.
- 315 Kort, A., Ouf, F. X., Gelain, T., Malet, J., Lakhmi, R., Breuil, P., and Viricelle, J. P.: Quantification of soot deposit on a resistive sensor: Proposal of an experimental calibration protocol, *J. Aerosol Sci.*, 156, 105783, <https://doi.org/10.1016/j.jaerosci.2021.105783>, 2021.
- 320 Kort, A., Ouf, F. X., Lakhmi, R., Gelain, T., Malet, J., Breuil, P., and Viricelle, J. P.: An innovative method for soot deposit quantification using a CO<sub>2</sub> sensor: Application to fire studies in research facilities, *J. Aerosol Sci.*, 164, <https://doi.org/10.1016/j.jaerosci.2022.106005>, 2022.
- Marhaba, I., Ferry, D., Laffon, C., Regier, T. Z., Ouf, F. X., and Parent, P.: Aircraft and MiniCAST soot at the nanoscale,  
325 *Combust. Flame*, 204, 278–289, <https://doi.org/10.1016/j.combustflame.2019.03.018>, 2019.
- Maricq, M. M.: Monitoring Motor vehicle pm emissions: An evaluation of three portable low-cost aerosol instruments, *Aerosol Sci. Technol.*, 47, 564–573, <https://doi.org/10.1080/02786826.2013.773394>, 2013.
- 330 Moore, R. H., Ziemba, L. D., Dutcher, D., Beyersdorf, A. J., Chan, K., Crumeyrolle, S., Raymond, T. M., Thornhill, K. L., Winstead, E. L., and Anderson, B. E.: Mapping the operation of the miniature combustion aerosol standard (Mini-CAST) soot generator, *Aerosol Sci. Technol.*, 48, 467–479, <https://doi.org/10.1080/02786826.2014.890694>, 2014.
- Ntziachristos, L., Giechaskiel, B., Ristimäki, J., and Keskinen, J.: Use of a corona charger for the characterisation of automotive  
335 exhaust aerosol, *J. Aerosol Sci.*, 35, 943–963, <https://doi.org/10.1016/j.jaerosci.2004.02.005>, 2004.
- Ntziachristos, L., Amanatidis, S., and Samaras, Z.: Application of the Pegasor Particle Sensor for the Measurement of Mass and Particle Number Emissions, *SAE Tech. Pap.*, 01, <https://doi.org/10.4271/2013-01-1561>, 2013.
- 340 Ouf, F. X., Parent, P., Laffon, C., Marhaba, I., Ferry, D., Marcillaud, B., Antonsson, E., Benkoula, S., Liu, X. J., Nicolas, C., Robert, E., Patanen, M., Barreda, F. A., Sublemontier, O., Coppalle, A., Yon, J., Miserque, F., Mostefaoui, T., Regier, T. Z.,



- Mitchell, J. B. A., and Miron, C.: First in-flight synchrotron X-ray absorption and photoemission study of carbon soot nanoparticles, *Sci. Rep.*, 6, <https://doi.org/10.1038/srep36495>, 2016.
- 345 Ouf, F. X., Bourrous, S., Fauvel, S., Kort, A., Lintis, L., Nuvoli, J., and Yon, J.: True density of combustion emitted particles: A comparison of results highlighting the influence of the organic contents, *J. Aerosol Sci.*, 134, 1–13, <https://doi.org/10.1016/j.jaerosci.2019.04.007>, 2019.
- Pandis, S. N., Baltensperger, U., Wolfenbarger, J. K., and John, H. S.: Inversion of aerosol data from epiphaniometer, *J. Aerosol Sci.*, 22, 417–428, 1991.
- 350
- Park, K., Kittelson, D. B., and McMurry, P. H.: Structural properties of diesel exhaust particles measured by Transmission Electron Microscopy (TEM): Relationships to particle mass and mobility, *Aerosol Sci. Technol.*, 38, 881–889, <https://doi.org/10.1080/027868290505189>, 2004.
- 355
- Rostedt, A., Arffman, A., Janka, K., Yli-Ojanperä, J., and Keskinen, J.: Characterization and response model of the PPS-M aerosol sensor, *Aerosol Sci. Technol.*, 48, 1022–1030, <https://doi.org/10.1080/02786826.2014.951023>, 2014.
- Weingartner, E., Saatho, H., Schnaiter, M., and Streit, N.: Absorption of light by soot particles : determination of the absorption coefficient by means of aethalometers, 34, 1445–1463, [https://doi.org/10.1016/S0021-8502\(03\)00359-8](https://doi.org/10.1016/S0021-8502(03)00359-8), 2003.
- 360